European Commission

JRC TECHNICAL REPORTS

Visual assessment of the Green European Settlement Map

Exploration and quality performance measures of the green component derived from the ESM algorithm

Maria PAFI, Stefano FERRI, Alice SIRAGUSA, Matina HALKIA

2016

EUR 28026 EN

This publication is a Technical report by the Joint Research Centre, the European Commission's in-house science service. It aims to provide evidence-based scientific support to the European policy-making process. The scientific output expressed does not imply a policy position of the European Commission. Neither the European Commission nor any person acting on behalf of the Commission is responsible for the use which might be made of this publication.

Contact information
Name: Stefano FERRI
Address: Joint Research Centre, Via E. Fermi 2749, I-21027 Ispra (VA) Italy, TP 267
E-mail: stefano.ferri@jrc.ec.europa.eu
Tel.: +39 0332 786751

JRC Science Hub
https://ec.europa.eu/jrc

JRC102520

EUR 28026

ISBN 978-92-79-60072-2 (PDF)
ISBN 978-92-79-60073-9 (print)

ISSN 1831-9424 (online)
ISSN 1018-5593 (print)

doi:10.2788/601488 (online)
doi:10.2788/913829 (print)

How to cite: Maria PAFI, Stefano FERRI, Alice SIRAGUSA, Matina HALKIA; Visual assessment of the Green European Settlement Map. Exploration and quality performance measures of the green component derived from the ESM algorithm; EUR 28026; doi:10.2788/601488

Table of contents

Abstract

The urban green is currently at the core of scientific interest and policy-making in urban planning. The importance of the urban green component of the European Settlement Map (ESM) increases under the light of the absence of a homogenous layer in such coverage and resolution to be used in urban analysis.

The ESM, the first European Map of the built-up, was initially published in July 2014. It is part of the URBA project initiated by the Joint Research Centre and funded by the Directorate-General for Regional and Urban Policy (DG REGIO). In the beginning, the ESM was not intended to provide a green layer. However, the urban green gradually started receiving increasing interest from the users of the ESM. Since there were spectral bands available in the Copernicus Core 003 dataset on which the ESM was adopted, eventually the green component was integrated with the built-up.

This report addresses the quality assessment of the urban green component of the ESM defining thresholds over common vegetation indexes. The main purpose is to present reliable information about the dataset and test the possibility to move towards a new enhanced product if necessary, by deploying a post-processing method to decrease errors of omission and/or commission.

1. Introduction

Data for the monitoring of urban development and the comparison of urban patterns across cities are very limited, even for the member states of the European Union. This void has been largely filled by the release of the European Settlement Map (ESM), based on the Global Human Settlement Layer (GHSL) technology [1], [2]. However, the validation of specific components of the ESM has yet to be implemented in order to provide users with the necessary metadata.

Urban green is hard to define and thus hard to measure and model. The challenge we are addressing is dual: a) to explore the types of urban green detected by the ESM and b) to establish a robust methodology to evaluate this green detection. These two issues are difficult to address since there are numerous parameters to be taken into consideration.

Since the urban green influences many aspects of both natural environment and social life, it allows a multi-disciplinary approach. From a planning point of view, urban green has a more functionally-oriented connotation. It is a land use rather than a land cover. In this context, the public character of urban green is specifically significant, since it is considered to contribute to the quality of life [1]. However, since the ESM is derived by processing satellite images, the definition of urban green is strongly correlated with the presence of chlorophyll.

This technical report describes the experiment of complementing what remains in the urban space after the exclusion of the built-up and the streets, as defined by the European Settlement Map (ESM) methodology. This remaining space, namely open or unbuilt space, needs to be further explored in order to define its character and provide a useful tool for spatial scientists and policy-makers. It is within this open space that a category of particular interest can be traced. This category of open urban space is the so called "urban green".

2. Data

2.1 Dataset

The urban green layer is a component of the ESM. As described by [3] the ESM is the first European Map of the built-up, initially published in July 2014. It is part of the URBA project initiated by the Joint Research Centre and funded by the Directorate-General for Regional and Urban Policy (DG REGIO). In the beginning, the ESM was not intended to provide a green layer. The component of green was used as a mask to pre-process the data before the application of the main morphological analysis through which the component of the built-up was derived. However, gradually the urban green started receiving increasing interest from the users of the ESM. Since there were spectral bands available in the Copernicus Core 003 dataset on which the ESM was adopted, eventually the green component was integrated with the built-up.

The urban green layer was validated using the Copernicus Core_003 SPOT 5-6 dataset. This dataset is delivered in the Copernicus project for Earth Observation, contains 3.800 scenes at 2.5 m. resolution, 3 spectral bands namely NIR (near infrared band), RED (red band), GREEN (green band) and constitutes the highest resolution dataset available at the moment. The dataset is available as a pan-sharpening information product. The pan sharpening process is not well documented since, the parameters necessary for the calibration, namely the *gain* and the *offset*, are missing for the Red and Green bands. [4] [5].

2.2 Case study

The visual assessment is limited to a sample of the dataset covering the 28 EU Capitals (Figure 1). This technical report describes the first experiments on exploring and assessing the green component and constitutes part of an on-going project which will extend until 2017. Therefore, we define a relatively small sample for the beginning in order to test if the methodology applied could be replicable and valid for the future. We consider that the European capitals are a valid sample to start with, being typical representatives of each country since:

a) They usually accumulate the majority of the population

b) Their size, diversity of development modes render them more possible to cover the majority of urban typologies that can be observed in every country

Consecutively, we developed an extended sample of 100 settlements covering from large and medium – sized cities to small towns all across the European continent. This sample was assessed by two visual interpreters. However, the results of this sample will be part of a future paper.

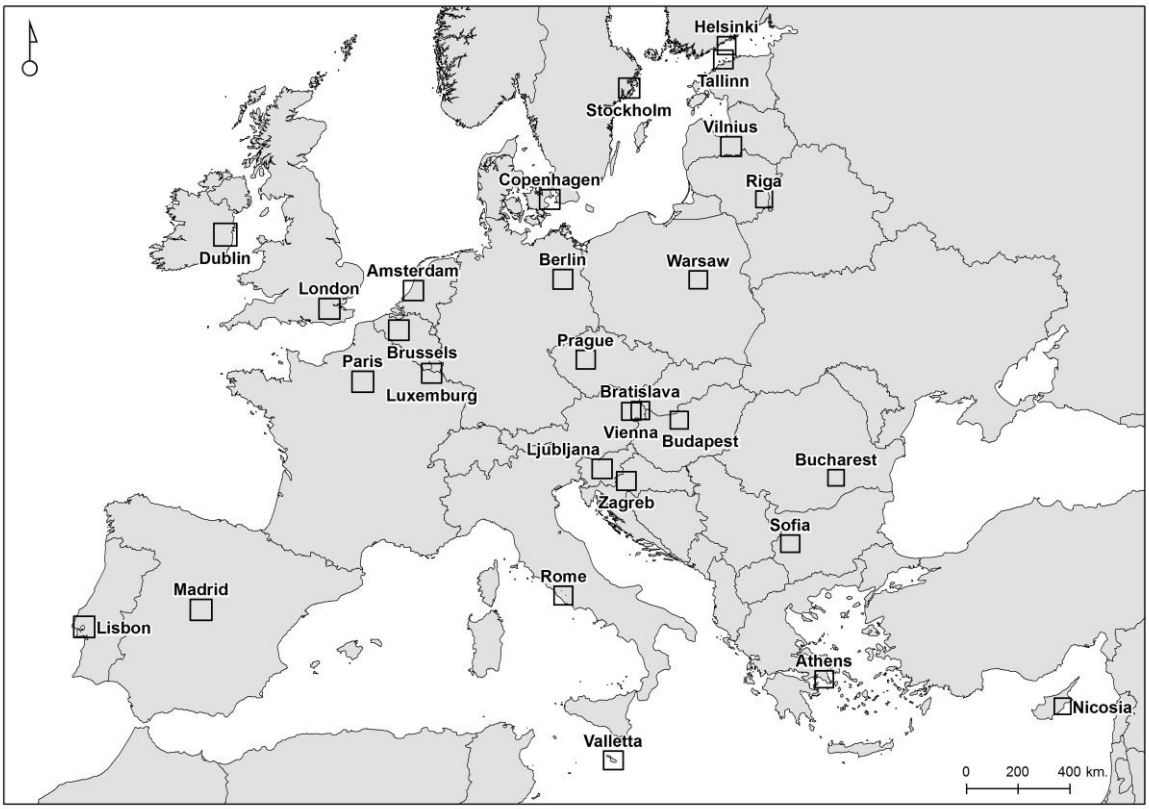

Figure 1: The case study (vector national borders added, Source: Eurostat 2014)

3. Method

The difficulty in establishing a pre-defined pure approach in assessing such an unbalanced component as the urban green and especially with non-calibrated data imposed a step-by-step approach. Instead of a sole method, we address two different experiments.

More specifically, both of the experiments implement thresholds over vegetation indexes based on the image histogram and adjusted via visual interpretation. The main difference lies in the fact that the first one defines thresholds on a very common vegetation index, namely the Normalised Difference Vegetation Index (NDVI), while the second one implements an adjusted index called pseudo NDVI ($NDVI_x$). Another difference regards the way the samples are selected in each satellite image before deciding the final threshold. These issues are addressed in detail in the following chapters.

Eventually, the green extracted through this thresholding method is used as ground truth layer to compare with the methodology refined by the Corine Land Cover (CLC) components as applied by [3]. The comparison among these two different green layers is applied using a set of well documented performance metrics.

The rationale behind the selection of a human validator to conduct the visual assessment is the human ability to use content and logic while toggling among several categories of classification [6] [7]. It was observed that specific types of green, such as grass, bushes, scrub, sparsely vegetated areas and clusters of all-year trees, do not demonstrate consistent signal behaviour. This kind of vegetation is hard to sufficiently quantify using automatic methods. Consequently, it is basically this type of urban green that the human interpreter is better at detecting in comparison with an unsupervised classification.

For the assessment we used the false colour band combination (123) images of SPOT 5 (Figure 2). This specific assignment of bands to channels represents vegetation in shades of red. Since plants tend to absorb the visible solar radiation (especially the red and blue radiation) and scatter solar radiation in the near-infrared part of the spectrum, they obtain the highest value in this specific spectral area which is allocated to the Red channel. Similarly, the artificial environment is a combination of materials which tend to reflect radiation in the visible spectrum. Thus, urban areas tend to obtain a pallet of different colours ranging from white (equal contribution of all bands) to cyan (combination of Green and Blue channels to which the visible bands of the red and green are correspondingly allocated).

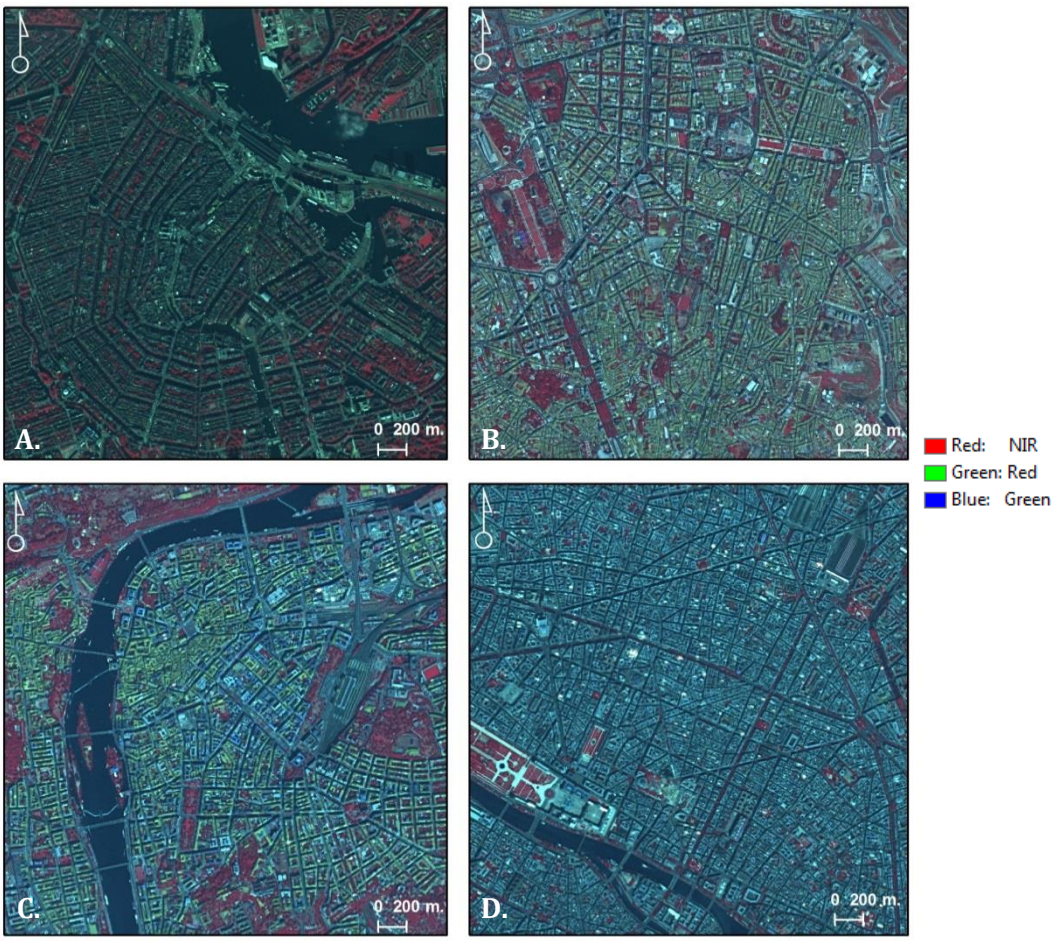

Figure 2 : RGB False colour band combination composites of the Copernicus_003 dataset. A. Amsterdam, B. Lisbon C. Prague, D. Paris

3.1 Vegetation Indexes

The well-documented Normalized Difference Vegetation Index (NDVI) was initially calculated for each of the 28 case studies according to formula [1].

$$\mathbf{NDVI} = \frac{NIR - RED}{NIR + RED} \ [\mathbf{1}]$$

In standard conditions, a NDVI value for vegetation would range from 0.3 to 0.8, with larger values representing the 'greener' areas, while bare soils typically range around 0.2-0.3. Healthy vegetation reflects intensely in the near infrared field of the spectrum. However, within the context of the missing gain and offset metadata of Red and Green during the procedure of pan-sharpening of the images, as well as the fact that the pan-sharpening itself was not documented, the standard values mentioned above cannot be referred to in this case. The threshold of 0.3 to discriminate the green from the non-green areas is not the case here. The loss of spectral information implies that the real reflectance of the image was also lost.

Ferri et al. (2014) developed a modified NDVI ($NDVI_x$) [2] in an effort to address this issue. This index implements one basic transformation of the three bands. More specifically, the maximum of the two visible bands (Red and Green), namely luminance (*L)*, is used to replace the red band (*RED*) of the standard NDVI [1] as a way to empirically enhance the built-up detection [4] [5].

$$\mathbf{NDVIx} = \frac{NIR - L}{NIR + L} \; [2]$$

After applying this luminance correction, linear rescale and casting were performed as described by [3].

The methodology developed here uses both these indexes in an effort to also assess their performance and open a discussion.

3.2 Performance Measures

The performance measures (i.e. measures, accuracy measures or measures of agreement) include a combination of 'traditional' evaluation measures and some techniques which were originally initialised for other purposes (ROC, Kappa etc.) but are highly recommended in filling the voids of the first ones. The reason is that traditional evaluation measures (Error Rates, Accuracy, Recall, Precision and F-measure) are not free of biases, thus receiving noticeable critical evaluation. Besides, deploying a multiple measure system is beginning to become quite typical since it offers the opportunity to reveal both the key advantages and the restrictions of the model [8].

The assessment is based on indicators originating from the contingency table (Table 1) referred also as confusion matrix .

Table 1: Example of a confusion matrix

	Condition «Gold standard» positive	**Condition «Gold standard» negative**	
Prediction positive	True Positive (TP)	False Positive (FP)	Predicted Positive (PP = TP+FP)
Prediction negative	False Negative (FN)	True Negative (TN)	Predicted Negative (PN = FN+TN)
	Real Positive (RP = TP+FN)	Real Negative (RN = FP+TN)	Total population (N = TP+FP+FN+TN)

Table 2 provides a brief description of the measures used. The order of the list is based on a logical sequence in order to minimise the calculations needed for the algorithm.

Table 2: Performance measures used for the analysis: An overview

Measure	Formula	Use
Bias (Label)	**Bias** = $\frac{PP}{N} = \frac{TP+FP}{N}$	• A measure to describe the distribution of the dataset (balanced or unbalanced)
Prevalence (Prev)	**Prev** = $\frac{RP}{N} = \frac{TP+FN}{N}$	• It describes a proportion (typically expressed as a percentage) • A measure of asymmetry
Sensitivity *(True Positive Rate – TPR, Recall)*	**TPR** = $\frac{TP}{RP} = \frac{TP}{TP+FN}$	• Proportion of Real Positive cases that are correctly Predicted Positive • Focuses only on the positive predictions (TN ignored)
Specificity *(True Negative Rate – TNR, Inverse Recall)*	***TNR*** = $\frac{TN}{RN} = \frac{TN}{FP+TN}$	• Proportion of Real Negative cases that are correctly Predicted Negative
Precision *(Positive Predictive Value – PPV,* ***User's accuracy****)*	**PPV** = $\frac{TP}{PP} = \frac{TP}{TP+FP}$	• Proportion of Predicted Positive cases that are correctly Real Positives • Focuses only on the positive predictions (TN ignored)
Inverse Precision *(Negative Predictive Value – NPV)*	**NPV** = $\frac{TN}{PN} = \frac{TN}{TN+FN}$	• Proportion of Predicted Negative cases that are indeed Real Negatives
Accuracy	**ACC** = $\frac{TP+TN}{N}$ = 2TPR × Prev + 1 − Bias − Prev	• It is one of the most common formulas in literature. However, it is highly influenced by unbalanced datasets
Balanced Accuracy	**BA** = $\frac{TPR+TNR}{2}$	• AUC for single prediction point • Better suited for unbalanced datasets than common ***Accuracy***
Informedness[1] *(Powers Kappa)*	**Informedness** = TPR + TNR – 1 = (TPR – Bias) / (1 – Prev)	• The probability that the prediction method will make a correct decision as opposed to guessing (bookmaker algorithm) • Better suited for unbalanced datasets
Kappa coefficient *(Cohen's Kappa)*	$\kappa^2 = \frac{p_o - p_e}{1 - p_e} = \frac{2(TP \times TN - FP \times FN)}{(TP+FN)(FN+TN)+(TP+FP)(FP+TN)}$	• A measure of inter-agreement. • A more robust measure than simple accuracy, since it takes into account the agreement occurring by chance.
F-score *(F –measure)*	$\mathbf{F_1} = 2\frac{PPV \times TPR}{PPV+TPR} = \frac{2TPR \times Prev}{Bias+Prev}$	• Harmonic mean of recall and precision • Focuses only on the positive predictions (TN ignored)
Mathew's correlation coefficient	$\mathbf{MCC} = \frac{TP \times TN - FP \times FN}{\sqrt{(TP+FP)(TP+FN)(TN+FP)(TN+FN)}}$	• A measure of quality of a binary (two-class) classification • A dichotomous of Pearson correlation, also known as ***φ (phi) coefficient***. • Balanced measure and one of the best in describing the confusion matrix

[1] A Kappa-like measure initiated by [8]. It has the same context as Balanced Acc

[2] where p_0= relative observed agreement among raters

p_e= hypothetical expected probability of chance agreement =ETP+ETN=PP x RP +RN x PN

More specifically, the results are analysed using a set of performance measures on different zones (whole scene, ESM Built-Up, Urban Clusters[3], and High-Density Urban Clusters[4]). In the end, we present only the results on the ESM BU (Table 3).

Table 3: ESM classes definition and Raster Value (Ferri, 2016)

ESM Raster Value		Description
BU	50	BU Buildings
BU	45	BU Area–Street Green NDVIx
BU	41	BU Area–Urban Atlas Green
BU	40	BU Area–Green NDVIx
BU	35	BU Area–Streets
BU	30	BU Area–Open Space
NBU	25	NBU Area–Street Green NDVIx
NBU	20	NBU Area–Green NDVIx
NBU	15	NBU Area–Streets
NBU	10	NBU Area–Open Space
	2	Railways
	1	Water
	0	No Data

3.3 Method 1

The assessment chain includes the following steps:

1. Definition of the 28 Copernicus SPOT 5 satellite images that provide the best coverage of each EU capital
2. Calculation of standard NDVI index (NDVI)
3. Recognition of urban green typologies (Figure 4)
4. Definition of thresholds over the NDVI based on histogram and visual adjustments
5. Vegetation extraction using the thresholds applied in Step 4 as follows: ***VEG=NDVI>Threshold***
6. Comparison with vegetation extracted by the model described by [3]: Calculation of accuracy measures and analysis of the results

The initial approach adopted a pixel-to-pixel juxtaposition between the initial SPOT 5 image and the NDVI focusing on the built areas of the image. After selecting what was considered as optimum threshold to discriminate vegetation based on the frequency histogram, a careful visual inspection of the image was applied. In the cases the interpreter was not confident in accurately classifying green or non-green, high resolution imagery was used as ancillary data.

[3] As developed and agreed by DG for Regional Policy, DG for Agriculture and Rural Development, Eurostat and JRC (2010)
[4] OECD and the DG for Regional Policy (2011)

The method of thresholding in image segmentation is widely used in the field of remote sensing [9] [8] [10] [11]. There have been developed methods for automatic selection, namely the Laplacian method [10], valley sharpening techniques, histogram stretching, the Otsu thresholding method etc. [12]. All of them are based on the histogram of frequencies. In the ideal case of a bimodal histogram with a deep and sharp valley between two peaks, the optimum threshold is usually detected near the bottom of the valley [10] [12]. However, in the majority of cases the histogram is not easy to interpret. Especially, in cases where the valley is flat, contains noise or there are many peaks and valleys, the selection of a threshold is not easy. Even when the histogram is almost bimodal, the optimum threshold might not be at the bottom of the valley (Figure 3).

This is the main reason this experiment is performed using a human interpreter instead of an algorithm that would automatically allocate a threshold. The visual image interpretation method is also well documented in literature [13] [9]. However, the description of the exact process a human validator follows in order to take the final decision for the threshold is not well described in the majority of the cases. Thus, it could be argued that the selection of the threshold is a very objective process. Since there is no "goodness" measure to evaluate any threshold, the objectivity of an automatic method could also be challenged as objective.

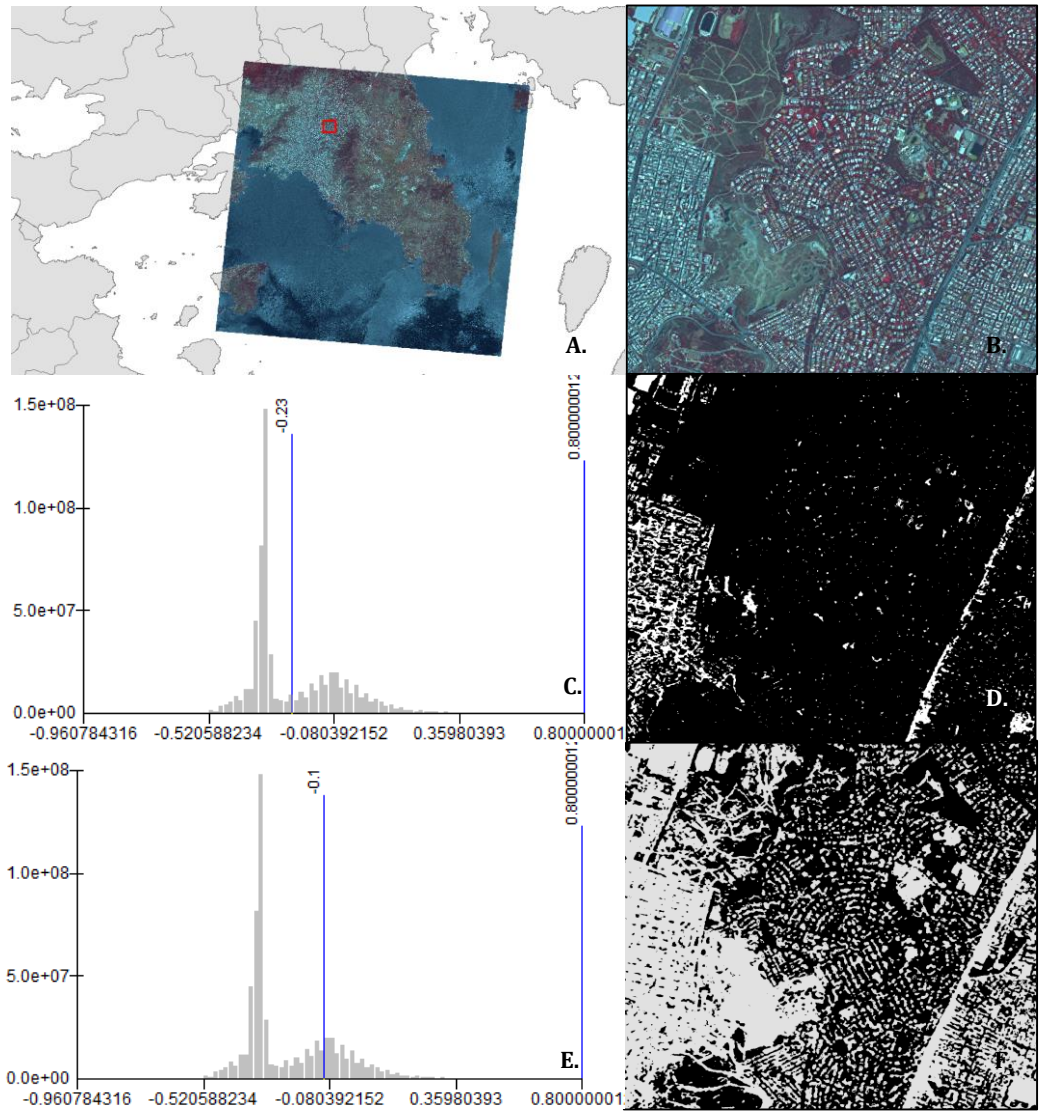

Figure 3: A. SPOT 5 False colour image of Athens, B. Zoom-in area, C. Threshold 1 selected at the bottom of the histogram valley, D. Green obtained with threshold 1 , E. Threshold 2 adjusted by visual validator, F. Green obtained with threshold 2

The focusing regions for defining the threshold were randomly selected, each time based on the specific characteristics of the satellite image. To better understand the extent of these regions imagine a moving window over the satellite image. The size of this window varies from bigger for non-urban to smaller for urban areas, where the spatial configuration of the green patches requires a finer resolution. The selection process followed a logical sequence:

a. Starting from rural areas where the open fields can easily be mistaken as green, the main focus was to find an initial threshold to discriminate them from fields containing vegetation (Figure 4A). This is essential in order to later avoid mistaking the open spaces of the city as urban green (Figure 4B). Still, the open spaces of a city are harder to track. So, the rural space served as a proxy for the selection of the first threshold.
b. Moving towards the urban core of the city, we focused on specific types of vegetation which we considered difficult to track. The explanation for this approach is that specific types of green that do not demonstrate consistent signal behaviour are hard to sufficiently quantify using any kind of automatic method. Such cases typically involve sparse vegetation near water bodies (Figure 4C), dry vegetation (Figure 4D), all-year trees with low emissions of chlorophyll (Figure 4E) and bushes-scrub (Figure 4F). Accordingly, we decreased the threshold in order to adjust it in such a way to adequately capture these cases as well.

Figure 4: Focusing regions on A. rural areas or suburbs, B. Open spaces within urban core, C. Sparse vegetation near water bodies, D. Dry vegetation E. All-year trees, F. Scrub and bushes

c. Toggling among the different possible thresholds deriving from the focusing areas, effort was made to mask the buildings out wherever feasible and to the extent that no evident influence occurs to the vegetation.

3.4 Method 2

Method 1 could be considered subjective in the selection of focusing areas for assessing the urban green and defining the optimum threshold. To mitigate this concern, a transition to a more robust framework was implemented. A hybrid sample-based approach was adopted for the assessment of the urban green detection. Instead of the concept of "focusing areas", which covered extended parts of the city, we initiated the widely used term of the "Region of Interest" (ROI). In remote sensing, ROIs are selected samples of a raster that are identical for a particular purpose. Usually, a ROI includes just few pixels in order to define consistent areas in terms of spectral information. Again, these ROIs were selected over patches of green that are difficult to capture by any algorithm.

More specifically, the validation chain includes the following steps:

1. Definition of the 28 Copernicus SPOT 5 satellite images that provide the best coverage of each EU capital (input from Method 1)
2. Recognition of urban green typologies across the cities (Figure 5)
3. Random sampling of ten (10) Regions of Interest (ROIs) within each city to cover all typologies of urban green, especially the lower marginal ones (dry green) that could be challenging for the algorithm to capture, but easier for the human eye to identify. Still, these areas are of great importance. Therefore, it would be an invaluable asset for the ESM to be able to capture these areas as well. Even if the ESM method does not sufficiently quantify these typologies of green, it still has to be checked whether it tracks the location of these areas.

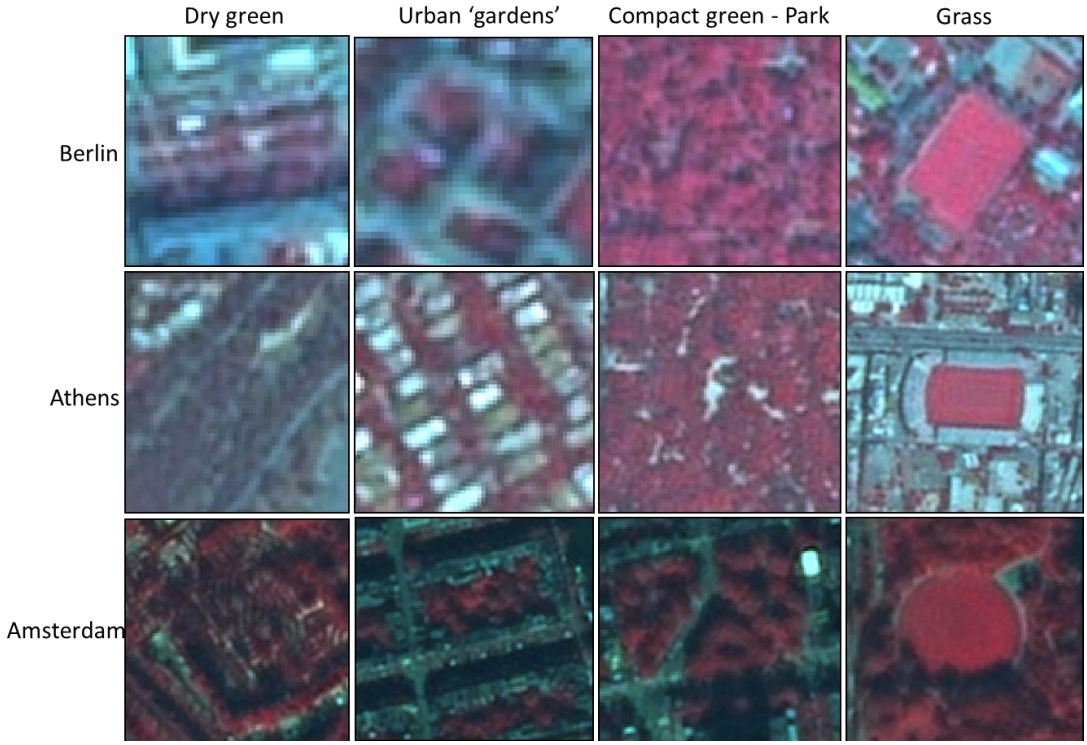

Figure 5: Urban green typologies

4. Calculation of the pseudo NDVI index ($NDVI_x$)
5. Average operator over the ROIs and $NDVI_x$

6. Definition of thresholds over the $NDVI_x$ obtained by average operator over the ROIs and subsequently visual adjustment
7. Vegetation extraction using the thresholds applied in Step 4 as follows: ***VEG= $NDVI_x$>Threshold***
8. Calculation of correlation coefficient (R^2) between NDVI and $NDVI_x$ to check the linear correlation of the two indexes (Table 4).
9. Comparison with vegetation extracted by the model described by Ferri (2016): Calculation of accuracy measures and analysis of the results

It is easier to select a threshold within an integer dataset rather than a floating type dataset, which is the case for the $NDVI_x$ after the rescaling, no other big improvement was observed in comparison to the standard NDVI, at least at first sight. Especially, in urban areas it is not easy to adequately separate the vegetation from the built-up just using only spectrally based indexes, because of a complex mixture of surface conditions. However, the luminance correction of the $NDVI_x$, still needs to be further analysed in order to provide a solid physical explanation for the reasons it was used instead of an already existent index.

The $NDVI_x$ could also be challenged for not being well-documented in literature. To mitigate this concern, the R^2 correlation coefficient was calculated for all the EU capitals (applied to the whole image). As can be seen in Table 4, a strong linear correlation does exist (minimum R^2 = 0.90).

Table 4: NDVI and $NDVI_x$ correlation coefficient

City	Country	R^2
Berlin	Germany	1.00
Rome	Italy	1.00
Lisbon	Portugal	1.00
Athens	Greece	1.00
Sofia	Bulgaria	1.00
Madrid	Spain	1.00
Tallinn	Estonia	1.00
Helsinki	Finland	0.99
London	United Kingdom	0.99
Valletta	Malta	0.99
Amsterdam	The Netherlands	0.99
Stockholm	Sweden	0.99
Copenhagen	Denmark	0.99
Vienna	Austria	0.99
Luxembourg	Luxembourg	0.99
Dublin	Ireland	0.98
Paris	France	0.98
Brussels	Belgium	0.97
Zagreb	Croatia	0.97
Budapest	Hungary	0.97
Vilnius	Lithuania	0.97
Bratislava	Slovakia	0.97
Bucharest	Romania	0.96
Nicosia	Cyprus	0.94
Riga	Latvia	0.93
Ljubljana	Slovenia	0.92
Prague	Czech Republic	0.91
Warsaw	Poland	0.90

4. Results

The results of the NDVI thresholds are presented and discussed below (Table 5). The list of the samples selected in order to obtain the average NDVI [$NDVI_x$ avg.] to be used as a starting point for the definition of the final threshold is presented in Figure 8.

Table 5: $NDVI_x$ thresholds

		Method 1	Method 2		
City	**Country**	**NDVI**	**NDVIx (ROIs avg.)**	**NDVIx final (visually adjusted)**	**Difference**
Amsterdam	The Netherlands	-0.15	51	48	3
Athens	Greece	-0.08	48	46	2
Berlin	Germany	-0.06	49	47	2
Bratislava	Slovakia	-0.05	50	49	1
Brussels	Belgium	-0.08	51	49	2
Bucharest	Romania	-0.15	50	48	2
Budapest	Hungary	-0.12	50	49	1
Copenhagen	Denmark	-0.10	46	46	0
Dublin	Ireland	-0.15	49	48	1
Helsinki	Finland	-0.06	49	46	3
Lisbon	Portugal	-0.10	50	48	2
Ljubljana	Slovenia	-0.28	45	45	0
London	United Kingdom	-0.15	47	46	1
Luxembourg	Luxembourg	-0.18	48	45	3
Madrid	Spain	-0.02	49	48	1
Nicosia	Cyprus	-0.02	53	50	3
Paris	France	-0.12	46	45	1
Prague	Czech Republic	-0.10	48	46	2
Riga	Latvia	0.35	-	-	-
Rome	Italy	-0.19	47	45	2
Sofia	Bulgaria	-0.02	49	47	2
Stockholm	Sweden	-0.30	44	44	0
Tallinn	Estonia	-0.05	52	49	3
Valletta	Malta	0.05	51	50	1
Vienna	Austria	-0.08	51	49	2
Vilnius	Lithuania	-0.12	48	48	0
Warsaw	Poland	-0.10	45	44	1
Zagreb	Croatia	-0.15	50	48	2

More specifically, the average value over the average values of the $NDVI_x$ obtained by the ROIs was tested as the first possible threshold and then visual assessment was conducted in order to validate this threshold. As can be seen in Figure 6, the selection of the average value of the ROIs as a threshold, (Th_{avg} = 47) is not always effective. For example, in the case of Athens, if the avg. of the ROIs is selected (Th_{avg} = 48), then the whole hill of Lycabettus –one of the most important green areas in Athens- is not included as urban green. If the ROIs minimum threshold is applied (Th_{min} = 44), then

areas that contain lots of vegetation (i.e. the municipality of Paleo Psychiko) tend to overestimate this vegetation covering all the open spaces and part of the buildings as well.

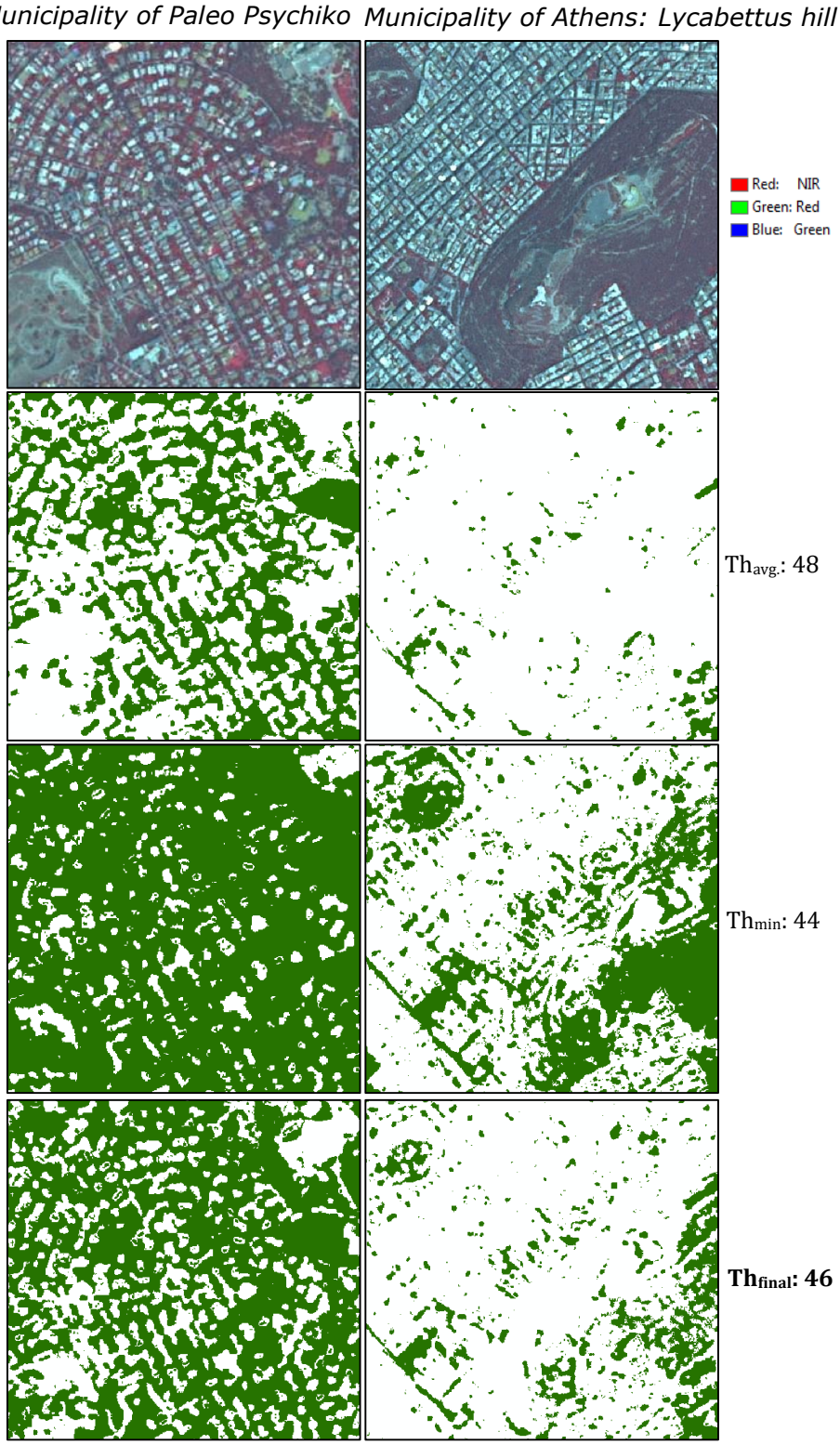

Figure 6: Process of threshold definition for Athens

On the contrary, Rome seems to be more resistant to changes in thresholds (Figure 7). However, the average ROIs threshold is still not the optimum one. Especially, in the historical centre, applying the Th_{avg} = 47 is inadequate for capturing the "urban gardens", meaning the green located within the urban blocks.

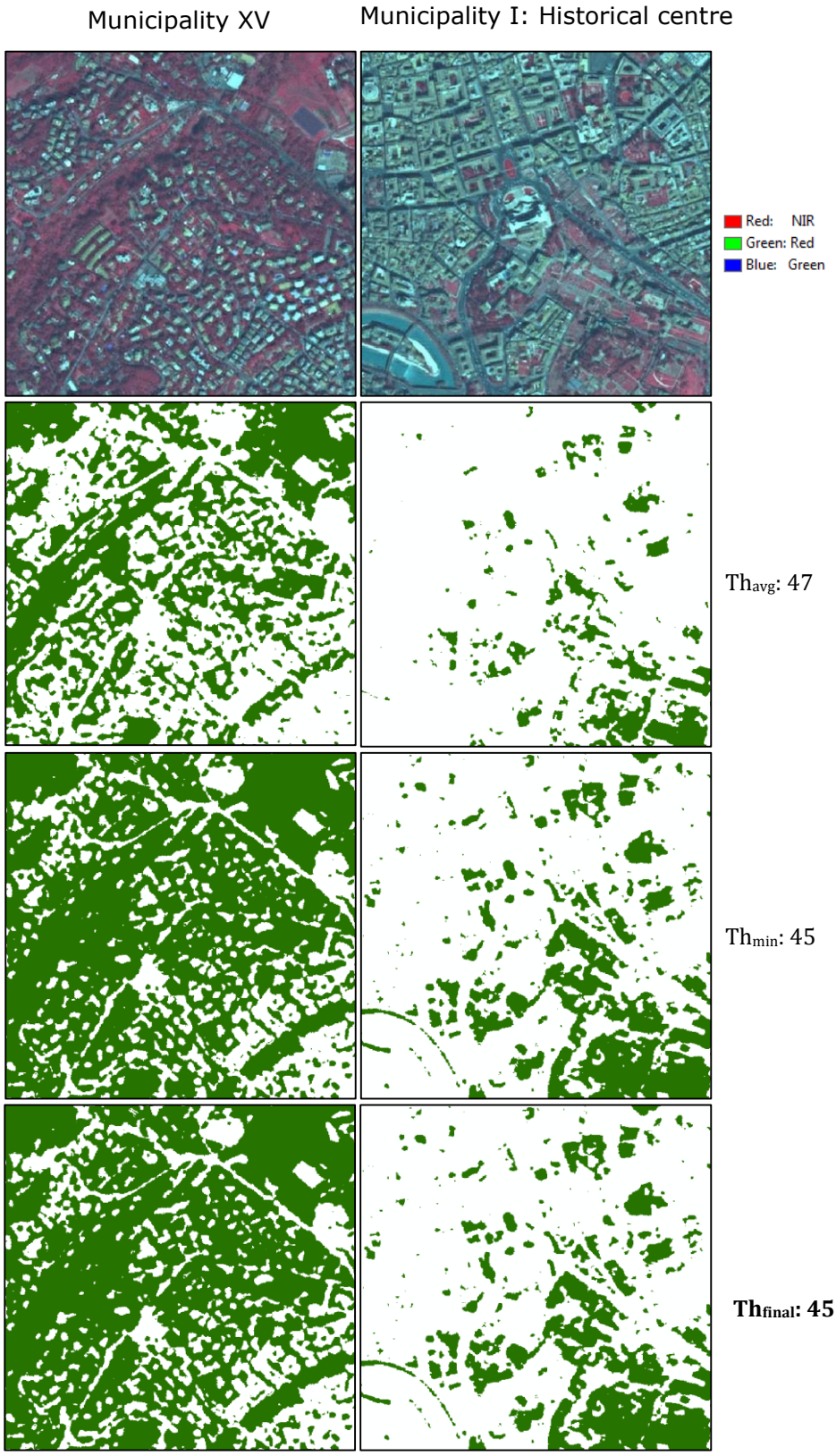

Figure 7: Process of threshold definition for Rome

ATHENS	
ROI	Avg. NDVIx
1	47
2	48
3	49
4	48
5	49
6	48
7	47
8	49
9	47
10	46
avg	47.8
std.dv	1.03
min	46
max	49

AMSTERDAM	
ROI	Avg. NDVIx
1	57
2	46
3	51
4	53
5	49
6	55
7	51
8	51
9	53
10	48
avg	51.4
std.dv	3.27
min	46
max	57

BERLIN	
ROI	Avg. NDVIx
1	49
2	46
3	47
4	46
5	56
6	48
7	49
8	47
9	56
10	50
avg	49.4
std.dv	3.72
min	46
max	56

BRATISLAVA	
ROI	Avg. NDVIx
1	50
2	52
3	48
4	52
5	53
6	52
7	53
8	49
9	50
10	51
avg	51
std.dv	1.70
min	48
max	53

BRUSSELS	
ROI	Avg. NDVIx
1	52
2	52
3	51
4	47
5	50
6	55
7	48
8	50
9	50
10	49
avg	50.4
std.dv	2.27
min	47
max	55

BUDAPEST	
ROI	Avg. NDVIx
1	52
2	50
3	51
4	51
5	51
6	51
7	48
8	53
9	52
10	49
avg	50.8
std.dv	1.48
min	48
max	53

BUCHAREST	
ROI	Avg. NDVIx
1	49
2	49
3	48
4	51
5	52
6	49
7	51
8	50
9	50
10	51
avg	50
std.dv	1.25
min	48
max	52

BUCHAREST	
ROI	Avg. NDVIx
1	45
2	45
3	46
4	46
5	45
6	43
7	46
8	48
9	46
10	47
avg	45.7
std.dv	1.34
min	43
max	48

DUBLIN	
ROI	Avg. NDVIx
1	48
2	49
3	48
4	49
5	51
6	51
7	48
8	48
9	48
10	48
avg	48.8
std.dv	1.23
min	48
max	51

HELSINKI	
ROI	Avg. NDVIx
1	51
2	51
3	51
4	51
5	50
6	50
7	49
8	48
9	44
10	48
avg	49.3
std.dv	2.21
min	44
max	51

LISBON	
ROI	Avg. NDVIx
1	47
2	49
3	49
4	50
5	48
6	51
7	50
8	52
9	50
10	51
avg	49.7
std.dv	1.49
min	47
max	52

LJUBLJIANA	
ROI	Avg. NDVIx
1	44
2	46
3	45
4	44
5	44
6	45
7	45
8	44
9	45
10	45
avg	44.7
std.dv	0.67
min	44
max	46

LONDON	
ROI	Avg. NDVIx
1	47
2	45
3	49
4	48
5	46
6	47
7	47
8	50
9	47
10	46
avg	47.2
std.dv	1.48
min	45
max	50

LUXEMBOURG	
ROI	Avg. NDVIx
1	47
2	49
3	48
4	48
5	48
6	49
7	49
8	48
9	46
10	48
avg	48
std.dv	0.94
min	46
max	49

MADRID	
ROI	Avg. NDVIx
1	50
2	52
3	48
4	48
5	49
6	51
7	50
8	49
9	50
10	47
avg	49.4
std.dv	1.51
min	47
max	52

NICOSIA	
ROI	Avg. NDVIx
1	52
2	54
3	54
4	53
5	54
6	52
7	51
8	54
9	50
10	54
avg	52.8
std.dv	1.48
min	50
max	54

PARIS	
ROI	Avg. NDVIx
1	47
2	47
3	45
4	46
5	46
6	48
7	46
8	45
9	46
10	47
avg	46.3
std.dv	0.95
min	45
max	48

PRAGUE	
ROI	Avg. NDVIx
1	47
2	47
3	49
4	47
5	49
6	50
7	49
8	50
9	48
10	48
avg	48.4
std.dv	1.17
min	47
max	50

ROME	
ROI	Avg. NDVIx
1	46
2	45
3	47
4	46
5	47
6	48
7	47
8	46
9	45
10	48
avg	46.5
std.dv	1.08
min	45
max	48

SOFIA	
ROI	Avg. NDVIx
1	49
2	48
3	49
4	49
5	50
6	50
7	49
8	49
9	49
10	49
avg	49.1
std.dv	0.57
min	48
max	50

STOCKHOLM	
ROI	Avg. NDVIx
1	45
2	47
3	42
4	44
5	44
6	41
7	45
8	42
9	42
10	44
avg	43.6
std.dv	1.84
min	41
max	47

TALLIN	
ROI	Avg. NDVIx
1	54
2	52
3	52
4	53
5	50
6	54
7	53
8	52
9	50
10	52
avg	52.2
std.dv	1.40
min	50
max	54

VIENNA	
ROI	Avg. NDVIx
1	52
2	51
3	52
4	54
5	52
6	51
7	50
8	52
9	49
10	51
avg	51.4
std.dv	1.35
min	49
max	54

VALLETTA	
ROI	Avg. NDVIx
1	50
2	52
3	52
4	52
5	52
6	50
7	50
8	52
9	51
10	53
avg	51.4
std.dv	1.07
min	50
max	53

VALLETTA	
ROI	Avg. NDVIx
1	50
2	48
3	47
4	48
5	47
6	48
7	47
8	49
9	48
10	48
avg	48
std.dv	0.94
min	47
max	50

WARSAW	
ROI	Avg. NDVIx
1	47
2	43
3	45
4	44
5	42
6	43
7	47
8	43
9	45
10	46
avg	44.5
std.dv	1.78
min	42
max	47

ZAGREB	
ROI	Avg. NDVIx
1	50
2	51
3	50
4	49
5	50
6	49
7	48
8	50
9	51
10	52
avg	50
std.dv	1.15
min	48
max	52

Figure 8: List of ROIs selected per EU capital

The results provided below (Table 6 & **Error! Reference source not found.**) refer to the ESM zone defined by the classes 40, 41, 30 because this is the zone of practical interest for the evaluation. The ESM built-up has already been validated and is no further questioned. It is a rule of the ESM method that the built-up always overrides the green.

Thus, the exclusion of the built-up serves a dual purpose:

a) *theoretically,* the purpose of this report is to complement what remains in the urban space after the exclusion of built-up and streets.

b) *technically,* the exclusion of built-up reduces the commission error originating from very bright surfaces.

The results obtained by both methods indicated a general underestimation trend. The sensitivity analysis performed in a number of different zones, namely the whole scene, the ESM urban zone, urban clusters, and high-density urban clusters, revealed that despite some slight differentiations, the pattern is always consistent. The model under detects the vegetation as indicated by the omission errors and the subsequent decrease in the producer's accuracy rate. However, during the visual assessment it was observed that the model is efficient in tracking the location of the green.

This empirical observation can be verified by the high accuracy (ACC) and balanced accuracy (BA) rates for all 28 EU capitals. The Matthews correlation coefficient (MCC), which provides a condensed description of the confusion matrix, is always above zero (which stands for random possibility). In specific, the MCC ranges from 0.63 to 0.82 in method 1 and from 0.63 to 0.86 in method 2, implying a very satisfying classification.

The Kappa coefficient ranges from moderate (0.57) to strong agreement (0.82) for method 1, and similarly for method 2 (0.57 - 0.86). The results do not significantly improve using the $NDVI_X$ instead of the standard NDVI (Table 6).

A comparative analysis of the results between *method 1* and *method 2* is provided in

Table 8, which constitutes a difference matrix. It is observed that the Accuracy and precision remain almost intact by the change in indexes. What is improved is the omission error in some cases, but at the same time commission error increases. This makes it even more difficult to understand the differences of the two vegetation indexes.

Table 6: Performance measures using the standard NDVI - Method 1

City	ACC	BA	Informedness	TPR	TNR	NPV	F1	MCC	Kappa	Commission Error	Omission Error	Producer Acc	UserAcc
Amsterdam	0.96	0.86	0.72	0.74	0.98	0.98	0.74	0.72	0.72	0.26	0.26	0.74	0.74
Athens	0.99	0.70	0.40	0.40	1.00	0.99	0.57	0.63	0.57	0.01	0.60	0.40	0.99
Berlin	0.98	0.77	0.53	0.53	1.00	0.99	0.68	0.70	0.67	0.06	0.47	0.53	0.94
Bratislava	0.97	0.83	0.66	0.66	0.99	0.98	0.76	0.76	0.75	0.11	0.34	0.66	0.89
Brussels	0.97	0.79	0.58	0.59	1.00	0.97	0.72	0.73	0.71	0.06	0.41	0.59	0.94
Bucharest	0.93	0.73	0.47	0.47	1.00	0.93	0.64	0.66	0.60	0.01	0.53	0.47	0.99
Budapest	0.97	0.88	0.76	0.77	0.99	0.97	0.83	0.82	0.82	0.08	0.23	0.77	0.92
Copenhagen	0.96	0.79	0.58	0.59	1.00	0.97	0.72	0.72	0.70	0.07	0.41	0.59	0.93
Dublin	0.98	0.82	0.63	0.64	0.99	0.98	0.73	0.72	0.71	0.16	0.36	0.64	0.84
Helsinki	0.99	0.77	0.55	0.55	1.00	0.99	0.71	0.73	0.70	0.01	0.45	0.55	0.99
Lisbon	0.98	0.79	0.57	0.57	1.00	0.98	0.71	0.73	0.70	0.05	0.43	0.57	0.95
Ljubljana	0.97	0.77	0.54	0.54	1.00	0.97	0.68	0.69	0.66	0.09	0.46	0.54	0.91
London	0.97	0.82	0.63	0.63	1.00	0.97	0.76	0.76	0.74	0.05	0.37	0.63	0.95
Luxembourg	0.98	0.81	0.62	0.62	1.00	0.98	0.75	0.76	0.74	0.04	0.38	0.62	0.96
Madrid	0.95	0.81	0.61	0.62	1.00	0.95	0.76	0.76	0.73	0.02	0.38	0.62	0.98
Nicosia	0.97	0.80	0.59	0.60	1.00	0.98	0.71	0.72	0.70	0.11	0.40	0.60	0.89
Paris	0.95	0.80	0.61	0.61	1.00	0.95	0.75	0.75	0.72	0.03	0.39	0.61	0.97
Prague	0.98	0.81	0.62	0.62	1.00	0.98	0.75	0.76	0.74	0.05	0.38	0.62	0.95
Riga	0.97	0.83	0.66	0.66	1.00	0.97	0.80	0.80	0.78	0.00	0.34	0.66	1.00
Rome	0.98	0.87	0.73	0.74	0.99	0.99	0.76	0.75	0.75	0.23	0.26	0.74	0.77
Sofia	0.94	0.80	0.60	0.61	1.00	0.94	0.75	0.74	0.72	0.03	0.39	0.61	0.97
Stockholm	0.95	0.81	0.63	0.63	1.00	0.95	0.77	0.77	0.74	0.01	0.37	0.63	0.99
Tallinn	0.94	0.77	0.54	0.54	1.00	0.93	0.70	0.71	0.67	0.00	0.46	0.54	1.00
Valleta	0.96	0.76	0.52	0.52	1.00	0.96	0.68	0.70	0.66	0.01	0.48	0.52	0.99
Vienna	0.98	0.79	0.57	0.58	1.00	0.98	0.71	0.72	0.70	0.06	0.42	0.58	0.94
Vilnius	0.97	0.74	0.48	0.48	1.00	0.97	0.65	0.68	0.63	0.00	0.52	0.48	1.00
Warsaw	0.99	0.79	0.57	0.58	1.00	0.99	0.73	0.75	0.72	0.01	0.42	0.58	0.99

Table 7: Performance measures using the NDVIx - Method 2

City	ACC	BA	Informedness	TPR	TNR	NPV	F1	MCC	Kappa	Commission Error	Omission Error	Producer Acc	UserAcc
Amsterdam	0.98	0.89	0.78	0.78	1.00	0.98	0.87	0.86	0.86	0.03	0.22	0.78	0.97
Lisbon	0.97	0.76	0.51	0.51	1.00	0.97	0.68	0.70	0.66	0.01	0.49	0.51	0.99
Bucharest	0.97	0.78	0.56	0.56	1.00	0.97	0.69	0.69	0.67	0.12	0.44	0.56	0.88
Ljubljana	0.99	0.78	0.56	0.56	1.00	0.99	0.72	0.74	0.71	0.02	0.44	0.56	0.98
Budapest	0.97	0.82	0.65	0.65	1.00	0.97	0.76	0.76	0.75	0.08	0.35	0.65	0.92
Zagreb	0.97	0.78	0.55	0.55	1.00	0.97	0.71	0.72	0.69	0.02	0.45	0.55	0.98
Vienna	0.95	0.77	0.54	0.54	1.00	0.95	0.69	0.70	0.67	0.03	0.46	0.54	0.97
Dublin	0.95	0.81	0.63	0.63	1.00	0.95	0.77	0.77	0.74	0.01	0.37	0.63	0.99
London	0.98	0.81	0.61	0.62	0.99	0.98	0.72	0.72	0.71	0.13	0.38	0.62	0.87
Warsaw	0.96	0.88	0.77	0.80	0.97	0.99	0.69	0.67	0.66	0.40	0.20	0.80	0.60
Paris	0.97	0.80	0.59	0.60	0.99	0.97	0.70	0.70	0.68	0.16	0.40	0.60	0.84
Tallinn	0.99	0.78	0.57	0.57	1.00	0.99	0.68	0.69	0.67	0.15	0.43	0.57	0.85
Copenhagen	0.99	0.84	0.68	0.68	1.00	0.99	0.76	0.75	0.75	0.16	0.32	0.68	0.84
Luxembourg	0.98	0.79	0.57	0.57	1.00	0.98	0.71	0.73	0.70	0.06	0.43	0.57	0.94
Rome	0.95	0.79	0.58	0.58	1.00	0.94	0.73	0.73	0.70	0.01	0.42	0.58	0.99
Helsinki	0.98	0.82	0.63	0.64	0.99	0.98	0.70	0.69	0.69	0.22	0.36	0.64	0.78
Vilnius	0.97	0.87	0.74	0.74	0.99	0.97	0.83	0.82	0.81	0.07	0.26	0.74	0.93
Berlin	0.99	0.70	0.41	0.41	1.00	0.99	0.58	0.63	0.57	0.01	0.59	0.41	0.99
Madrid	0.97	0.81	0.61	0.62	0.99	0.98	0.70	0.69	0.69	0.20	0.38	0.62	0.80
Sofia	0.97	0.78	0.55	0.55	1.00	0.98	0.70	0.71	0.69	0.05	0.45	0.55	0.95
Athens	0.95	0.81	0.62	0.63	1.00	0.95	0.76	0.75	0.73	0.04	0.37	0.63	0.96
Bratislava	0.99	0.85	0.70	0.70	1.00	0.99	0.80	0.81	0.80	0.06	0.30	0.70	0.94
Prague	0.98	0.83	0.67	0.67	1.00	0.98	0.77	0.77	0.76	0.08	0.33	0.67	0.92
Brussels	0.97	0.90	0.80	0.82	0.98	0.98	0.81	0.79	0.79	0.19	0.18	0.82	0.81
Nicosia	0.94	0.80	0.60	0.60	1.00	0.94	0.74	0.73	0.71	0.04	0.40	0.60	0.96
Stockholm	0.96	0.79	0.58	0.58	1.00	0.96	0.71	0.71	0.69	0.08	0.42	0.58	0.92
Valletta	0.98	0.90	0.79	0.80	0.99	0.99	0.81	0.80	0.80	0.18	0.20	0.80	0.82

Table 8: Impact on performance measures applying Method 2

DIFFERENCE MATRIX														
City	Country	ACC	BA	Informedness	TPR	TNR	NPV	F1	MCC	Kappa	Commission Error	Omission Error	Producer Acc	UserAcc
Amsterdam	The Netherlands	0.02	0.03	0.06	0.04	0.02	0.00	0.13	0.14	0.14	-0.23	-0.04	0.04	0.23
Athens	Greece	0.02	0.06	0.11	0.11	0.00	0.02	0.11	0.07	0.09	0.00	-0.11	0.11	0.00
Berlin	Germany	0.01	0.01	0.03	0.03	0.00	0.02	0.01	0.01	0.00	0.06	-0.03	0.03	-0.06
Bratislava	Slovakia	0.02	-0.05	-0.10	-0.10	0.01	0.01	-0.04	-0.02	-0.04	-0.09	0.10	-0.10	0.09
Brussels	Belgium	0.00	0.03	0.07	0.06	0.00	0.00	0.04	0.03	0.04	0.02	-0.06	0.06	-0.02
Bucharest	Romania	0.04	0.05	0.08	0.08	0.00	0.04	0.07	0.06	0.09	0.01	-0.08	0.08	-0.01
Budapest	Hungary	-0.02	-0.11	-0.22	-0.23	0.01	-0.02	-0.14	-0.12	-0.15	-0.05	0.23	-0.23	0.05
Copenhagen	Denmark	0.01	0.02	0.05	0.04	0.00	0.02	0.05	0.05	0.04	-0.06	-0.04	0.04	0.06
Dublin	Ireland	0.00	-0.01	-0.02	-0.02	0.00	0.00	-0.01	0.00	0.00	-0.03	0.02	-0.02	0.03
Helsinki	Finland	-0.03	0.11	0.22	0.25	-0.03	0.00	-0.02	-0.06	-0.04	0.39	-0.25	0.25	-0.39
Lisbon	Portugal	-0.01	0.01	0.02	0.03	-0.01	-0.01	-0.01	-0.03	-0.02	0.11	-0.03	0.03	-0.11
Ljubljiana	Slovenia	0.02	0.01	0.03	0.03	0.00	0.02	0.00	0.00	0.01	0.06	-0.03	0.03	-0.06
London	United Kingdom	0.02	0.02	0.05	0.05	0.00	0.02	0.00	-0.01	0.01	0.11	-0.05	0.05	-0.11
Luxembourg	Luxembourg	0.00	-0.02	-0.05	-0.05	0.00	0.00	-0.04	-0.03	-0.04	0.02	0.05	-0.05	-0.02
Madrid	Spain	0.00	-0.02	-0.03	-0.04	0.00	0.01	-0.03	-0.03	-0.03	-0.01	0.04	-0.04	0.01
Nicosia	Cyprus	0.01	0.02	0.04	0.04	-0.01	0.00	-0.01	-0.03	-0.01	0.11	-0.04	0.04	-0.11
Paris	France	0.02	0.07	0.13	0.13	-0.01	0.02	0.08	0.07	0.09	0.04	-0.13	0.13	-0.04
Prague	Czech Republic	0.01	-0.11	-0.21	-0.21	0.00	0.01	-0.17	-0.13	-0.17	-0.04	0.21	-0.21	0.04
Rome	Italy	0.00	-0.02	-0.05	-0.04	-0.01	0.01	-0.10	-0.11	-0.09	0.20	0.04	-0.04	-0.20
Sofia	Bulgaria	-0.01	-0.09	-0.18	-0.19	0.01	-0.01	-0.06	-0.04	-0.06	-0.18	0.19	-0.19	0.18
Stockholm	Sweden	0.01	0.01	0.02	0.02	0.00	0.01	0.01	0.01	0.01	0.01	-0.02	0.02	-0.01
Tallinn	Estonia	0.04	0.04	0.07	0.07	0.00	0.04	0.03	0.04	0.06	0.05	-0.07	0.07	-0.05
Valleta	Malta	0.04	0.06	0.13	0.13	0.00	0.05	0.07	0.06	0.09	0.08	-0.13	0.13	-0.08
Vienna	Austria	0.01	0.14	0.28	0.30	-0.02	0.02	0.13	0.09	0.13	0.18	-0.30	0.30	-0.18
Vilnius	Lithuania	-0.04	0.01	0.03	0.02	0.00	-0.04	0.03	0.01	0.01	-0.02	-0.02	0.02	0.02
Warsaw	Polonia	-0.01	0.05	0.10	0.10	0.00	-0.01	0.06	0.03	0.06	0.08	-0.10	0.10	-0.08
Zagreb	Croatia	-0.01	0.11	0.22	0.22	-0.01	0.00	0.08	0.05	0.08	0.17	-0.22	0.22	-0.17

4.1 A comparative analysis between vegetation indexes

A supplementary analysis on the behaviour of the two indexes is implemented using as case study the area of Athens. The concept of standard NDVI is well documented and has long been used in remote sensing. Given that the Near Infrared radiation of the vegetation is completely reflected and the Red radiation at the same time is entirely absorbed, this index provides a physical explanation for the detection of the vegetation.

As far as the $NDVI_x$ is concerned, the luminance correction incurs a different result in the cases where the Green is higher than the Red. This index is known as the GNDVI (Green Normalized Difference Vegetation Index) [14] and is calculated according to the following formula [3]:

$$\mathbf{GNDVI} = \frac{NIR - GREEN}{NIR + GREEN} \quad [3]$$

For the cases where the amount of the Red reflectance is equal or bigger than the Green, the $NDVI_x$ coincides with the standard NDVI. To visualise the areas in which these differences occur, a raster was created. It is obvious (Table 9) that in the majority of the cases (80%) the use of the NDVI prevails, while the GNDVI is mainly calculated for pixels that are saturated (very bright roofs etc.).

Table 9: $NDVI_x$ components Athens

Condition	Index used	Num. of pixels	Area (ha)	% of total area
Red > Green	NDVI	147.669.673	92.294	20%
Green > Red	GNDVI	578.200.879	361.376	80%

To obtain a better understanding of the performance of the two indexes, ten ROIs representing different typologies of land cover were selected. These ROIs served as zones to calculate the statistics for the indexes and create the following diagrams. The lines in these diagrams represent average, minimum and maximum NDVI and GNDVI curves. The purpose is to analyse the behaviour of the two indexes used to form the $NDVI_x$ and compare them with a number of other vegetation indexes available in literature (Table 10).

Table 10: List of vegetation spectral indices

Index	Source	Formula
DVI, Difference Vegetation Index	Tucker, 1979	NIR - red
GDVI, Green Difference Vegetation Index	Sripada et.al., 2006	NIR – green
GNDVI, Green Normalized Difference Vegetation Index	Buschmann and Nagel, 1993	(NIR – green) / (NIR + green)
NDVI, Normalized Difference Vegetation Index	Rouse, 1973	(NIR – red) / (NIR + red)
NG, Normalized Green	Sripada et al., 2006	Green / (NIR + red + green)
NR, Normalized Red	Sripada et al., 2006	Red / (NIR + red + green)
NNIR, Normalized Near Infrared	Sripada et al., 2006	NIR / (NIR + red + green)
RVI, Ratio Vegetation Index (also known as the Simple Ratio)	Birth and McVey, 1968	NIR / red
GRVI, Green Ratio Vegetation Index	Sripada et.al., 2006	NIR / green
VIgreen (VIg), Vegetation Index Green	Gitelson et al., 2002	(green – red) / (green + red)

Barzegar et.al (2015) explored different methods for extracting vegetation from semi-urban and agricultural regions, and compared the results using overall accuracy and the Kappa statistic. For this purpose, a combination of the aforementioned vegetation indexes was tested for three image datasets. Results revealed that DVI index can better detect vegetation [15].

As can be observed by the diagrams, and especially by the mean values (Diagram 1& Diagram 2), it is the behaviour of the NDVI rather than any other index that seems to follow a logical pattern. The sequence of the typologies, sorted from the highest to the lowest value of the NDVI, provides a smooth transition from healthy vegetation to artificial environment. The classes of dry vegetation, open fields, shrub and bushes and rock are ranked in the middle of the distribution. Given that it is within this range that the thresholds are approximately set to extract the vegetation. A small change in this typology sequence occurs by the GNDVI. It is not obvious if these changes are negative or not, but it is a fact that bushes and shrub and rock have the same value.

The majority of the other indexes present a non-linear behaviour. More specifically, the DVI which according to [15] performs better, in the image of Athens it lists the class "building with typical terrace" right after the class "dry trees". In this case, selecting a threshold smaller than zero would underestimate the green increasing omission errors, while in the opposite case the buildings would be mistaken as green increasing the commission errors.

Figure 9: Examples of ROIs in the image of Athens

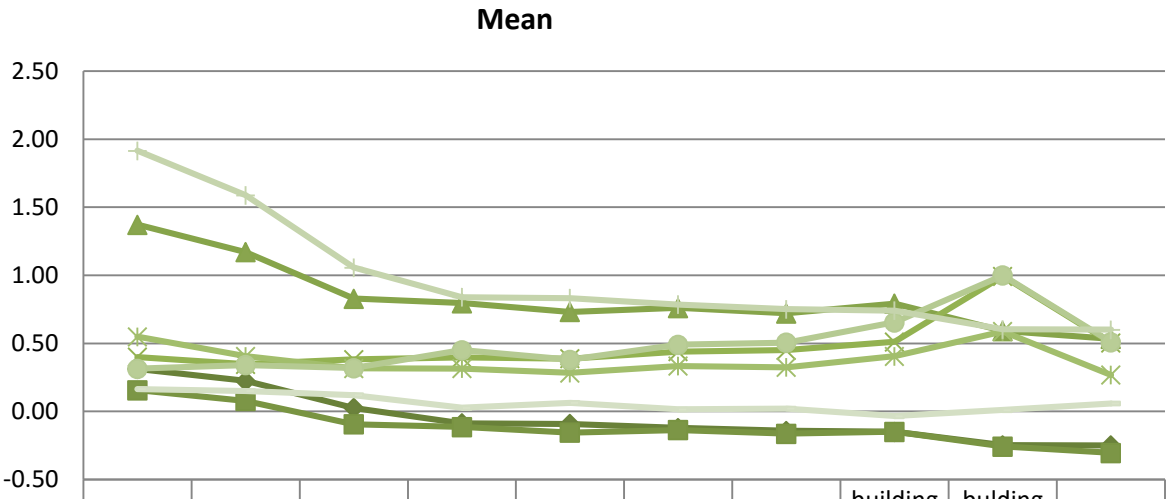

	healthy grass	healthy trees	dry trees	open fields	bushes and scrub	dry grass	rock	building with ceramic roof	bulding with typical terrace	parking lot
NDVI MEAN	0.31	0.23	0.03	-0.09	-0.09	-0.12	-0.14	-0.15	-0.25	-0.25
GNDVI	0.16	0.08	-0.09	-0.11	-0.16	-0.14	-0.16	-0.15	-0.26	-0.30
GRVI MEAN	1.37	1.17	0.83	0.80	0.73	0.76	0.72	0.79	0.59	0.53
NG MEAN	0.40	0.35	0.38	0.40	0.39	0.44	0.45	0.51	0.99	0.50
NNIR MEAN	0.55	0.41	0.32	0.32	0.28	0.33	0.33	0.41	0.59	0.27
NR MAX	0.31	0.34	0.32	0.45	0.38	0.49	0.51	0.65	1.00	0.51
RVI MEAN	1.92	1.59	1.06	0.84	0.83	0.79	0.75	0.74	0.60	0.60
Vig MEAN	0.16	0.15	0.12	0.03	0.06	0.02	0.02	-0.03	0.01	0.06

Diagram 1: Mean of normalised vegetation indexes

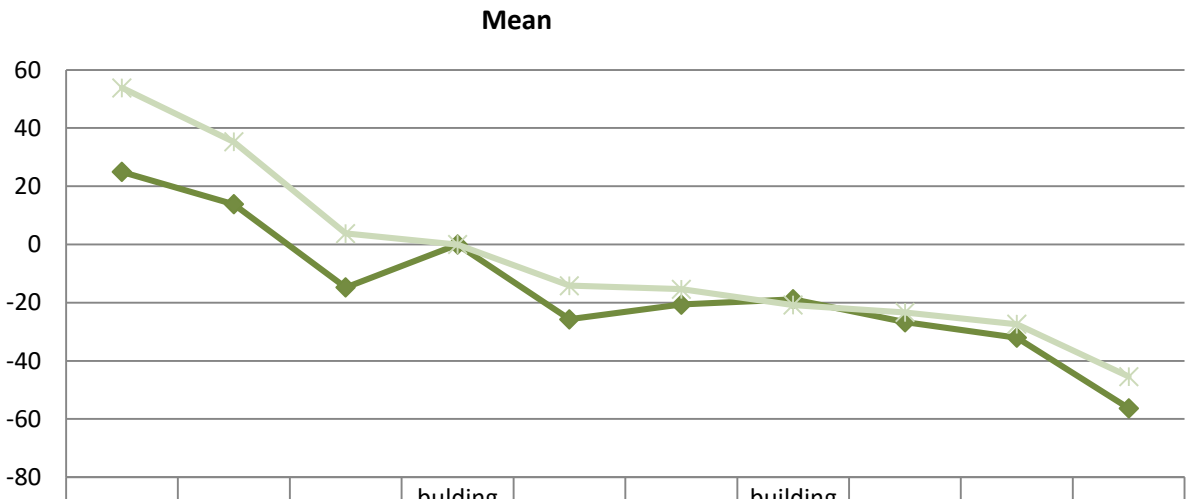

	healthy grass	healthy trees	dry trees	bulding with typical terrace	bushes and scrub	open fields	building with ceramic roof	dry grass	rock	parking lot
GDVI MEAN	25	14	-15	0	-26	-21	-19	-27	-32	-56
DVI MEAN	54	35	4	0	-14	-15	-21	-23	-27	-45

Diagram 2: Mean of vegetation indexes

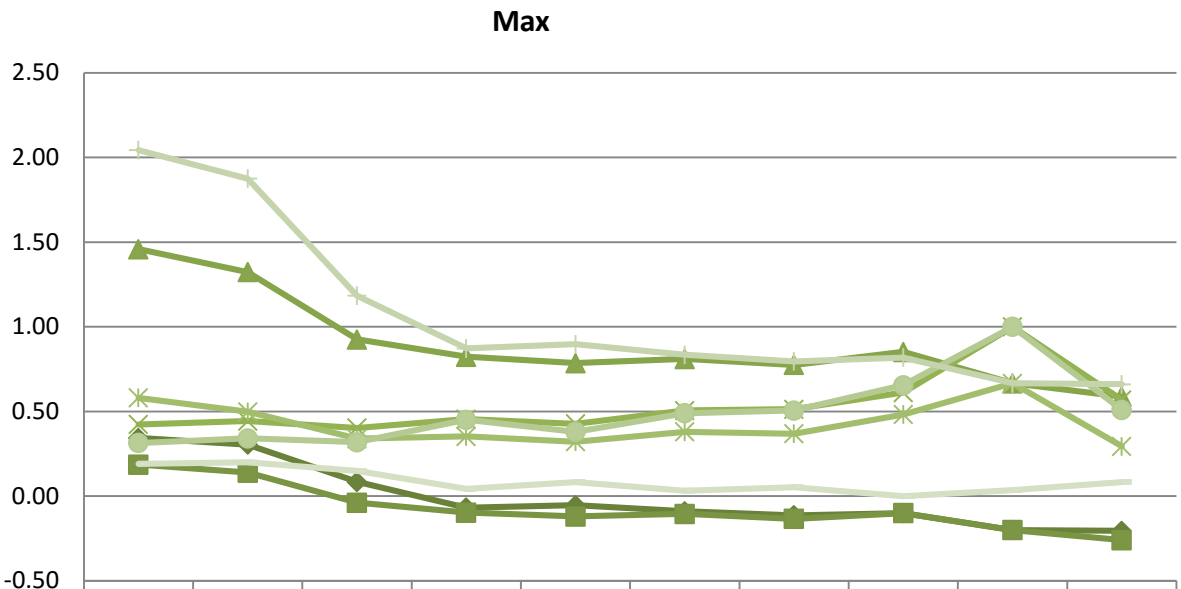

	healthy grass	healthy trees	dry trees	open fields	bushes and scrub	dry grass	rock	building with ceramic roof	bulding with typical terrace	parking lot
NDVI MAX	0.34	0.30	0.08	-0.07	-0.05	-0.09	-0.11	-0.10	-0.20	-0.20
GNDVI MAX	0.19	0.14	-0.04	-0.10	-0.12	-0.10	-0.13	-0.10	-0.20	-0.26
GRVI MAX	1.46	1.32	0.93	0.82	0.79	0.81	0.78	0.85	0.67	0.59
NG MAX	0.42	0.44	0.40	0.45	0.43	0.51	0.51	0.61	1.00	0.57
NNIR MAX	0.58	0.50	0.34	0.35	0.32	0.38	0.37	0.48	0.67	0.29
NR MAX	0.31	0.34	0.32	0.45	0.38	0.49	0.51	0.65	1.00	0.51
RVI MAX	2.04	1.88	1.18	0.87	0.90	0.84	0.80	0.82	0.67	0.66
Vig MAX	0.19	0.20	0.15	0.04	0.08	0.03	0.05	0.00	0.04	0.08

Diagram 4: Max of normalised vegetation indexes

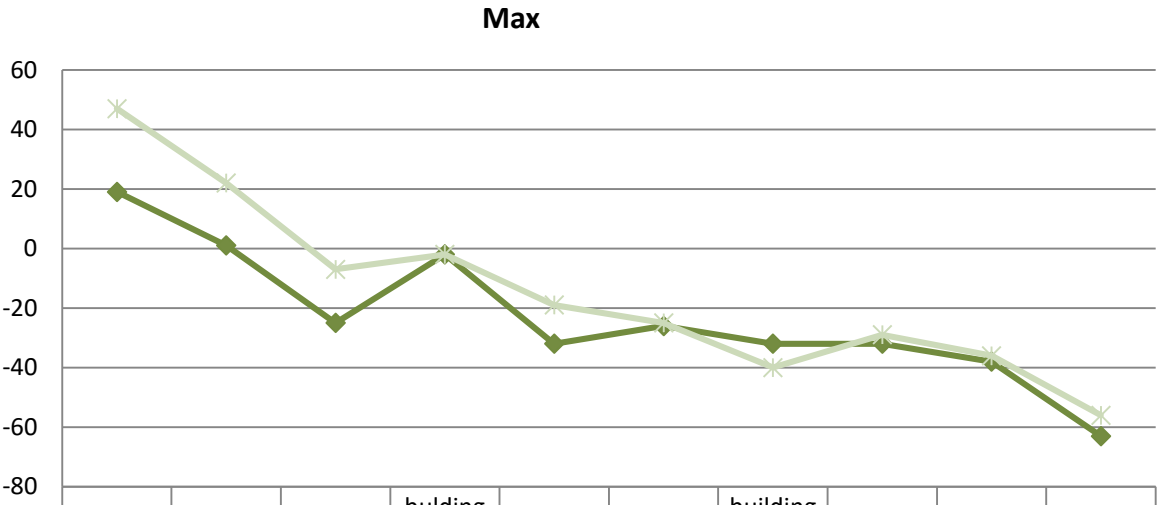

	healthy grass	healthy trees	dry trees	bulding with typical terrace	bushes and scrub	open fields	building with ceramic roof	dry grass	rock	parking lot
GDVI MIN	19	1	-25	-2	-32	-26	-32	-32	-38	-63
DVI MIN	47	22	-7	-2	-19	-25	-40	-29	-36	-56

Diagram 3: Max of vegetation indexes

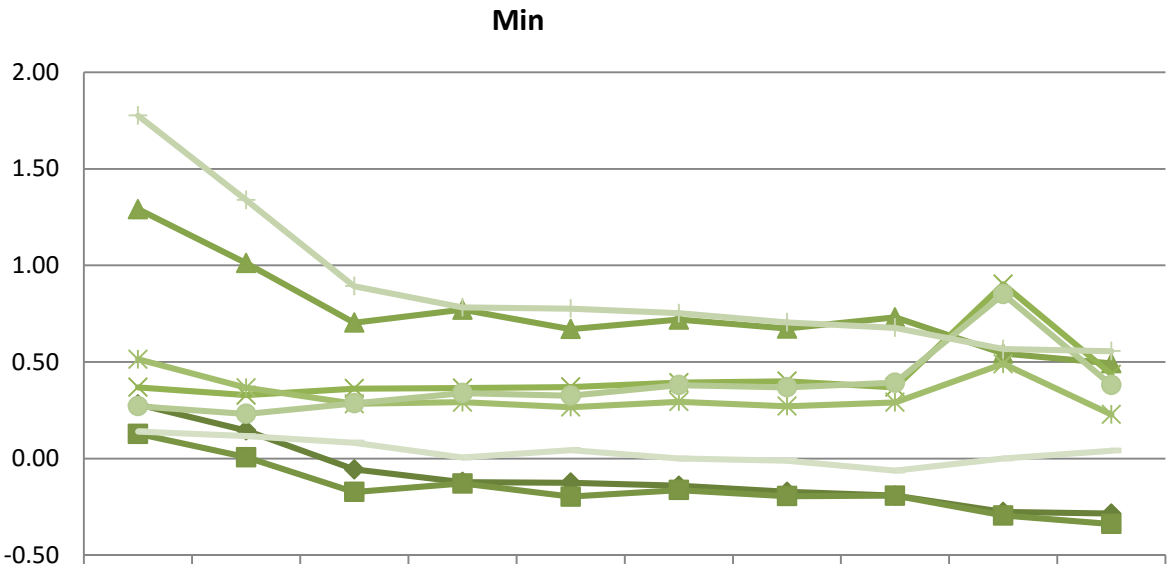

	healthy grass	healthy trees	dry trees	open fields	bushes and scrub	dry grass	rock	building with ceramic roof	bulding with typical terrace	parking lot
NDVI MIN	0.28	0.14	-0.06	-0.12	-0.13	-0.14	-0.17	-0.19	-0.28	-0.29
GNDVI MIN	0.13	0.01	-0.17	-0.13	-0.20	-0.16	-0.20	-0.19	-0.30	-0.34
GRVI MIN	1.29	1.01	0.70	0.77	0.67	0.72	0.67	0.73	0.54	0.49
NG MIN	0.37	0.33	0.36	0.36	0.37	0.39	0.40	0.37	0.90	0.44
NNIR MIN	0.51	0.37	0.28	0.29	0.27	0.29	0.27	0.29	0.49	0.23
NR MIN	0.27	0.23	0.29	0.34	0.33	0.38	0.37	0.39	0.85	0.38
RVI MIN	1.78	1.34	0.89	0.78	0.78	0.75	0.71	0.68	0.57	0.56
Vig MIN	0.14	0.12	0.08	0.00	0.04	0.00	-0.01	-0.06	0.00	0.04

Diagram 6: Min of normalised vegetation indexes

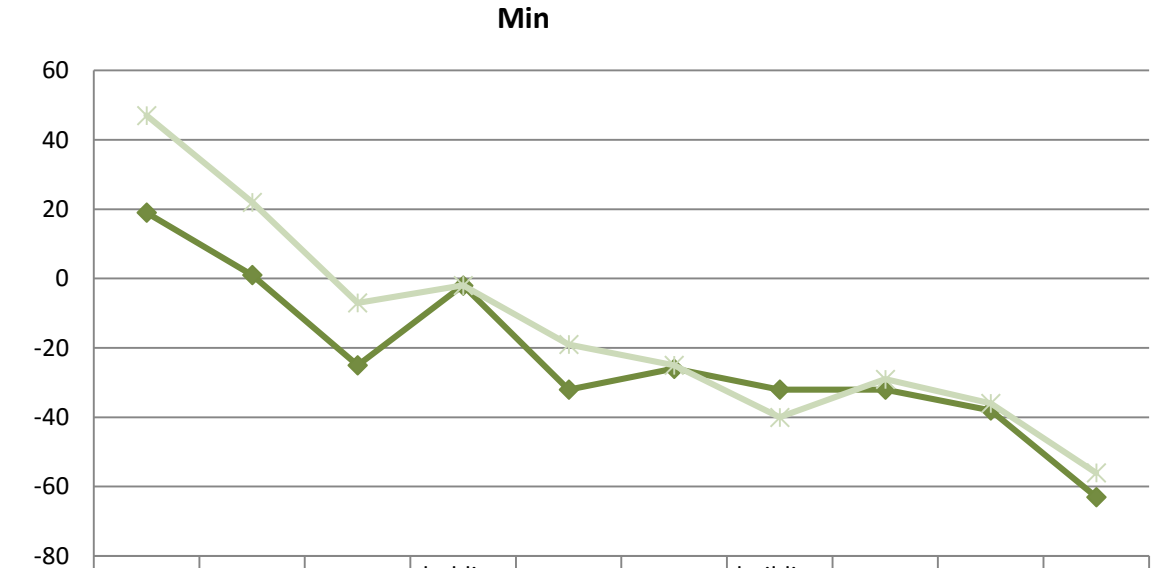

	healthy grass	healthy trees	dry trees	bulding with typical terrace	bushes and scrub	open fields	building with ceramic roof	dry grass	rock	parking lot
GDVI MIN	19	1	-25	-2	-32	-26	-32	-32	-38	-63
DVI MIN	47	22	-7	-2	-19	-25	-40	-29	-36	-56

Diagram 5: Min of vegetation indexes

5. Discussion

Some discussion points were developed through this procedure.

i) First, the inability to calibrate the raw data and the subsequent irregular behaviour of the majority of the vegetation indexes, pose restrictions that need to be kept into consideration.

ii) Second, applying a single threshold to capture the urban green in a whole city is a difficult task. Considering both the different configuration of green patches, related to the geographical location, and the different spectral behaviour of vegetation, highly dependent on the type and season of the year the image was obtained, it becomes obvious that the threshold applied is highly deviate. What is more, the atmospheric conditions can also alter the behaviour of the index. This combination of spatial, spectral and atmospheric parameters can highly explain the deviation of the thresholds among the EU capitals. What requires further explanation is the effect of the rescaling the $NDVI_x$ underwent. As it can be observed in Diagram 8, the rescaling poses an extreme non-linear behaviour to the dataset.

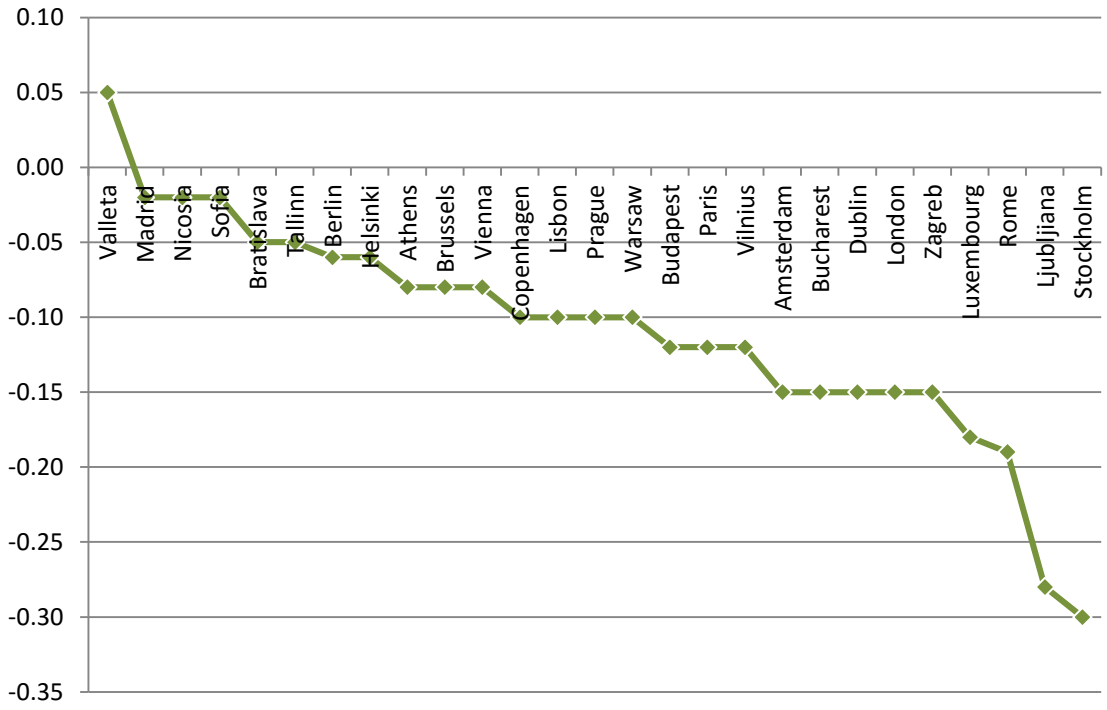

Diagram 7: Standard NDVI distribution of thresholds for the EU capitals

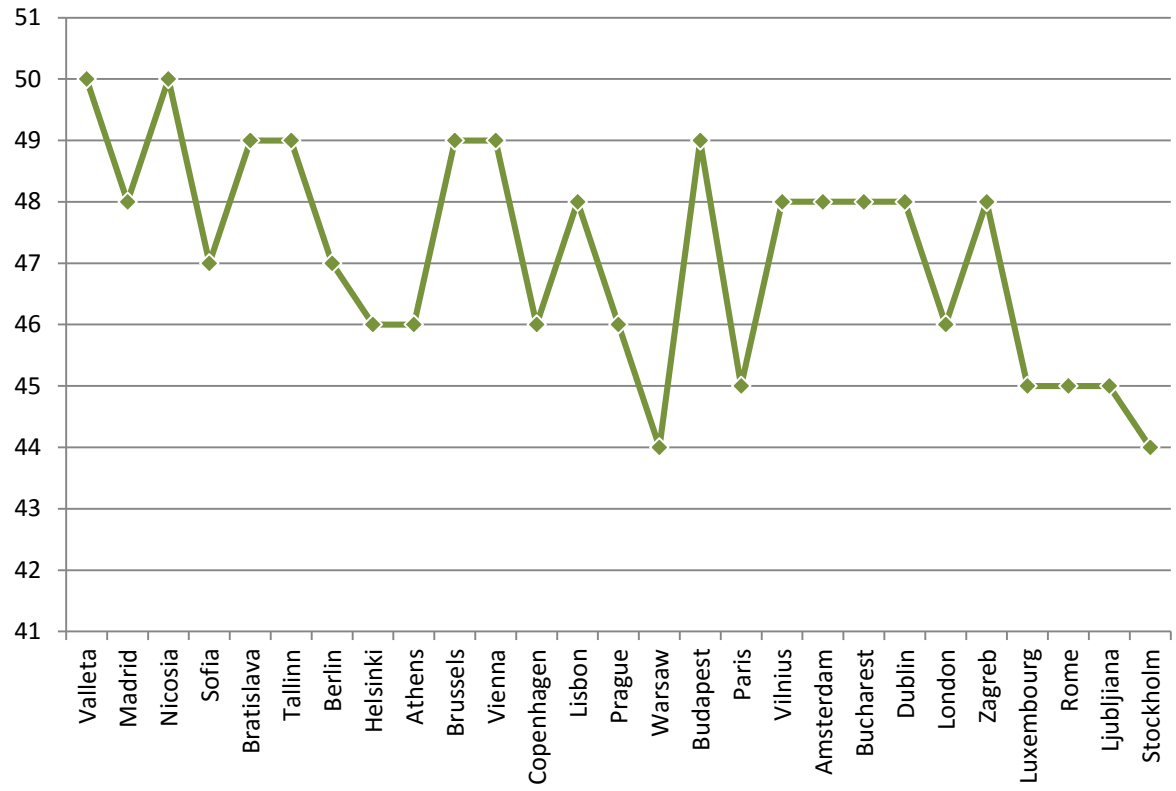

Diagram 8: NDVIx distribution of thresholds for the EU capitals

iii) Third, the validation was performed on the pan-sharpened image of 2.5 m. resolution making it easier for the human eye to detect the detailed boundary of the green area. Still, the spectral information remains at 5 m. resolution with all the biases occurring from the data manipulation process described previously. This in turn explains why the compact areas of healthy vegetation can be precisely mapped, while other types of green including all-year trees, scrub and bushes, dry grass and sparse vegetation, are tracked but not adequately depicted.

iv) Fourth, discussion point arises from the transition from method 1 to method 2. Assuming that the human interpreter has the ability to accurately select a representative set of sample areas (ROIs), then it can be stated that the second version constitutes a better approach. But then again, discussion would open as to how objective the validation is by using only one interpreter. It is true that a safer option would be to implement classification or segmentation on a dataset of high resolution images. But this method would only be applicable in a very small sample and at the same time.

v) The final discussion point regards the behaviour of both the NDVI and GNDVI which together constitute the pseudo NDVI ($NDVI_x$). The experiments and the analysis conducted failed to explain the advantages of using this complex index instead of one of those that already exists in literature. The luminance correction which the maximum operator applies in this case only affects the very bright saturated pixels for which the standard NDVI is long known not to operate well.

Conclusion

The visual assessment of the ESM green component conducted by defining thresholds on both the standard NDVI and the pseudo NDVI ($NDVI_x$) indexes revealed high accuracy and presicion and satisfying percentage of agreement, as indicated by the Kappa and Matthew's coefficients. The weak point of the dataset seems to be the underestimation of green, as proven by the ommission errors of average around 20%. Despite the possible restrictions of the assessment method, we feel that the approach is valid because the results can be plausible based on the visual inspection of the imagery. What could constitute a suggestion for a future release is the use of the standard NDVI rather than the pseudo NDVIx for the model. The fusion of two different indexes (NDVI and GNDVI) especially in a non-calibrated dataset makes the results difficult to analyse posing some additional irregularities in the distribution. Moreover, the way the NDVI is used in the concept of the $NDVI_x$ is the one that based on literature should be avoided, since this index does not perform well in saturated pixels.

References

[1] T. Morar, R. Radoslav, L. C. Spiridon and L. Păcurar, "Assessing pedestrian accessibility to green space using GIS," *Transylvania Review of Administrative Sciences,* vol. 42, no. E/2014, pp. 116-139, 2014.

[2] M. Pesaresi, G. Huadong, X. Blaes, D. Ehrlich, S. Ferri, L. Gueguen, M. Halkia, M. Kauffmann, T. Kemper, L. Lu, M. A. Marin-Herrera, G. K. Ouzounis, M. Scavazzon, P. Soille, V. Syrris and L. Zanchetta, "A Global Human Settlement Layer from Optical HR/VHR RS Data: Concept and First Results," *IEEE Journal of selected Topics in Applied Earth Observations and Remote Sensing,* vol. 6, no. 8, pp. 2102-2130, 2013.

[3] S. Ferri and M. Halkia, "The ESM green components: A dedicated focus on the production of the green in the European Settlement Map's workflow," EUR 28024. Ispra (Italy): Publications Office of the European Union; 2016. JRC102521. DOI: 10.2788/022426.

[4] S. Ferri, V. Syrris, A. J. Florczyk, M. Scavazzon, M. Halkia and M. Pesaresi, "A new map of the European Settlements by automatic classification of 2.5m resolution SPOT data," in *Proceedings IGARSS 2014*, Quebec, Canada, 2014.

[5] A. J. Florczyk , S. Ferri, V. Syrris, T. Kemper, M. Halkia, P. Soille and M. Pesaresi, "A New European Settlement Map From Optical Remotely Sensed Data," *IEEE Journal of Selected Topics in Applied Earth Observations and Remote Sensing,* vol. 9, no. 5, pp. 1978-1992, 2016.

[6] W.-C. Cheng, J.-C. Chang, C.-P. Chang, Y. Su and T.-M. Tu, "A Fixed – Threshold Approach to Generate High-Resolution Vegetation Maps for ICONOS Imagery," *Sensors,* vol. 8, no. 7, pp. 4308-4317, 2008.

[7] T. W. Lister, A. J. Lister and E. Alexander, "Land use change monitoring in Maryland using a probabilistic sample and rapid photointerpretation," *Applied Geography,* vol. 51, pp. 1-7, 2014.

[8] D. M. Powers, "The Problem with Kappa," in *Proceedings of the 13th Conference of the European Chapter of the Association for Computational Linguistics*, 2012.

[9] D. J. Nowak and E. J. Greenfield, "Evaluating The National Land Cover Database Tree Canopy and Impervious Cover Estimates Across the Conterminous United States: A Comparison with Photo-Interpreted Estimates," *Environmental Management,* vol. 46, no. 3, pp. 378-390, 2010.

[10] J. S. Weszka, R. N. Nagel and A. Rosenfeld, "A threshold selection technique," *IEEE Trans. Comput.,* Vols. C-23, pp. 1322-1326, 1974.

[11] C. Small, F. Pozzi and C. D. Elvidge, "Spatial analysis of global urban extend from DMSP-OLS night lights," *Remote Sensing of Environment,* vol. 96, pp. 277-291, 2005.

[12] N. Otsu, "A Threshold Selection Method from Grey-Level Histograms," *IEEE Transactions on Systems, Man and Cybernetics,* Vols. SMC-9, no. 1, pp. 62-66,

1979.

[13] T. R. Loveland, J. W. Merchant, D. O. Ohlen and J. F. Brown, "Development of a Land-Cover Characteristics Database for the Conterminous U.S," *Photogrammetric Engineering and Remote Sensing, Photogrammetric Engineering and Remote Sensing,* vol. 57, no. 11, pp. 1453-1463, 1991.

[14] C. Buschmann and E. Nagel, "In vivo spectroscopy and internal optics of leaves as basis for remote sensing of vegetation," *International Journal of Remote Sensing,* vol. 14, pp. 711-722, 1993.

[15] M. Barzegar, H. Ebadi and A. Kiani, "Comparison of different vegetation indices for very high-resolution images, specific case UltraCam-D imagery," *The International Archives of the Photogrammetry, Remote Sensing and Spatial Information Sciences,* Vols. XL-1/W5, 2015.

[16] L. Dijkstra and H. Poelman, "A harmonised definition of cities and rural areas: the new degree of urbanisation," Directorate-General for Regional and Urban Policy, 2014.

List of abbreviations and definitions

AOI	Area of Interest
CLC	Corine Land Cover
DG REGIO	Directorate-General for Regional and Urban Policy
ESM	European Settlement Map
EU	European Union
GHSL	Global Human Settlement Layer
GNDVI	Green Normalised Difference Vegetation Index introduced by Buschmann and Nagel (1993)
GREEN	Green band
NIR	Near Infrared band
NDVI	Normalised Difference Vegetation Index introduced by Rouse et.al. (1973)
$NDVI_x$	Pseudo Normalised Difference Vegetation Index introduced by the JRC (2015)
JRC	Joint Research Centre
RED	Red band
ROI	Region of Interest
BU	Built-Up. Built-up is any three dimensional manmade structure, fixed on the ground, that can hold people during day or night, occasionally or even sporadically (JRC, 2015)
Cities	Local administrative units with more than 50% of their population in an urban centre (http://epp.eurostat.ec.europa.eu/statistics_explained/index.php/Degree_of_urbanization_-_2011_revision)
Urban clusters	Clusters of contiguous (contiguity includes the diagonal) grid cells of 1 km^2 with a density of at least 300 inhabitants per km2 and a minimum population of 5.000 (DG REGIO, 2014)
High-density cluster (or city centre)	Contiguous grid cells of 1 km^2 with a density of at least 1.500 inhabitants per km^2 and a minimum population of 50.000 (DG REGIO, 2014)

List of figures

List of tables

List of diagrams

Europe Direct is a service to help you find answers to your questions about the European Union
Free phone number (*): 00 800 6 7 8 9 10 11
(*) Certain mobile telephone operators do not allow access to 00 800 numbers or these calls may be billed.

A great deal of additional information on the European Union is available on the Internet.
It can be accessed through the Europa server http://europa.eu

How to obtain EU publications

Our publications are available from EU Bookshop (http://bookshop.europa.eu),
where you can place an order with the sales agent of your choice.

The Publications Office has a worldwide network of sales agents.
You can obtain their contact details by sending a fax to (352) 29 29-42758.

LB-NA-28026-EN-N

JRC Mission

As the Commission's in-house science service, the Joint Research Centre's mission is to provide EU policies with independent, evidence-based scientific and technical support throughout the whole policy cycle.

Working in close cooperation with policy Directorates-General, the JRC addresses key societal challenges while stimulating innovation through developing new methods, tools and standards, and sharing its know-how with the Member States, the scientific community and international partners.

Serving society
Stimulating innovation
Supporting legislation

Publications Office

doi:10.2788/601488

ISBN 978-92-79-60072-2